Supporting Information

Espagne et al. 10.1073/pnas.1107272108

SI Materials and Methods

Cloning and Sequencing of *PaMe4* and *SME4* Genes. The *PaMe4* gene, which corresponds to the original Podospora *mei4-1* mutant allele (1–3), was identified by positional cloning. Correct identity of the cloned gene was confirmed in two ways. First, the *PaMe4* gene of the *mei4-1* mutant was sequenced; it differs from the isogenic WT allele by a single base change from C to T, which results in a nonsense mutation at position R460 (CGA to TGA) and predicts a truncated protein containing one-third of the WT length. Second, an ectopic insertion of the WT *PaMe4* gene restores WT sporulation to the *mei4-1* mutant. A list of microsatellites or SNP markers used for the cloning is available on request. PCR amplifications were done according to procedures developed for the *Podospora anserina* genome assembly (4). Transformation of the *mei4-1* mutant strain, which produces only few viable ascospores, was performed with a Podospora cosmid genomic DNA library of strain *S* (10 μg DNA of each cosmid). Complementation (restoration of sporulation) was obtained with cosmid 11H11. To further narrow the complementing sequence, we used two plasmids, GA0AB219BF04 and GA0AB328AF06, obtained by the genome-sequencing project. After cotransformation along with pBC-Hyg into the *mei4-1* mutant strain, the Hygromycin B-resistant transformants were crossed to the *mei4-1* mutant strain of the appropriate mating type. Only the Hygromycin B-resistant transformants issued from the transformation performed with plasmid GA0AB219BF04 showed clear restoration of ascospores. Each of the three predicted ORFs of plasmid GA0AB219BF04 was tested separately (details on request). One showed full complementation of the sporulation defect of *mei4-1*.

SME4 gene sequence (embl CABT01000092.1) was obtained from the *Sordaria macrospora* genome sequence (5) based on its sequence similarity with the *PaMe4* gene. The *SME4* DNA locus was sequenced de novo to correct the sequence, and the gene was reannotated manually using the cDNA sequence.

Deletion of PaMe4 and SME4. To construct the Δ*pame4::hygR* null allele, we amplified (by PCR) two 2-kb fragments corresponding to the 5′ *PaMe4* flanking sequence and the 3′ *PaMe4* flanking sequence using the pairs of primers Δpame1A (5′-aaAGATCTctcttgctgttgcagatgg-3′) and Δpame1B (5′-aagCGGCCGCacggtttgttgcttcagctc-3′) and Δpame2A (5′-aaTCTAGAcaccagactgcgatcagaaa-3′) and Δpame2B (5′-aaAGATCTcgagaatggaaagggtcaaa-3′), respectively, with *S*-strain genomic DNA as a template (details of PCR on request). The PCR amplified fragments were individually cloned into the pGEMT vector (Promega). The 2-kb 5′ *PaMe4* flanking sequence was released from the pGEMT vector using *Bgl*II and NotI (underlined in Δpame1A and Δpame1B sequences). The 2-kb 3′ *PaMe4* flanking sequence was released from the pGEMT vector using XbaI and *Bgl*II (underlined in Δpame2A and Δpame2B sequences). Both fragments were ligated to the pBC-hygro previously cleaved by NotI and XbaI. Transformation of the WT *S* strain was performed with 10 μg Δpa*me4::hygR* plasmid previously linearized at the unique *Bgl*II site to generate homologous recombination ends. Two Hygromycin B-resistant clones showed the expected sporulation-deficient phenotype when further crossed with a *PaMe4-1* mutant strain of appropriate mating type. One of the sterile transformants was selected for additional studies. Correct gene replacement of the *PaMe4*$^+$ WT allele by the Δpa*me4::hygR* mutant allele was verified by PCR and Southern blot analyses.

Mutant strains deleted for *SME4* were generated by gene substitution. The open-reading frame of *SME4* was replaced by the *Escherichia coli hph* gene conferring hygromycin resistance. The 5′ and 3′ flanking sequences were amplified using the following primers; for the 5′ flanking sequence, SME4-promxbaI 5′-TGCTCTAGACGGGTATGAAAGAGGTATCACAG-3′ and SME4-promhindIII 5′-CCCAAGCTTGTTGGGCACCTAGAGGCAAC-3′ primers were used, and for the 3′ flanking sequence, SME4-delTnotI 5′-ATAAGAATGCGGCCGCGTATGTGTGGTGTATTTGTCGGAG-3′ and SME4-delTxbaI 5′-TGCTCTAGAGTTACCTTTCGGGAGTCTAGCAAC-3′ were used. The 1,040-bp 3′ flanking sequence PCR-amplified fragment displays an XbaI restriction site at the 3′ end and a *Hind*III restriction site at the 5′ end (underlined nucleotides in the primers). The 869-bp 5′ flanking sequence PCR-amplified fragment displays a NotI restriction site in its 3′ end and an XbaI restriction site in its 5′ end (underlined nucleotides in the primers). Both fragments were ligated with the pBC-Hyg plasmid previously cleaved by *Hind*III and NotI. From this three-partner ligation experiment, we retrieved the ΔSme4::hygR plasmid harboring a complete deletion of the *SME4* protein coding sequence. The ΔSme4::hygR plasmid was linearized at the unique XbaI site to generate homologous recombination ends and was used for transformation of a *ku70*Δ mutant strain, which increases the homologous integration events. Transformants carrying a deleted allele were selected for hygromycin resistance and confirmed by PCR.

SME4-GFP Fusion. The GFP coding sequence (p-EGFP-1; Clontech) was fused to *SME4* just after the last C-terminal amino acid predicted from the *SME4* ORF. The ORF is amplified using primers SME4-prompst (5′-AACTGCAGGTCCTTCCTTCTT) and SME4-termsmaI (5′-TCCCCCGGGGATTTGTTGTCAGGCGGAGGA). Both PCR product and p-EGFP-1 were cleaved by *PstI* and *SmaI* and ligated using T4 DNA ligase (Fermentas). The GFP allele was ectopically integrated into a WT strain by cotransformation with pBC-nour. After selection for nourseothrycin resistance, transformants were screened for their expression of the Sme4-GFP fusion protein. Sme4-GFP was than introduced by genetic crosses into the *sme4Δ* strain. Sme4-GFP is fully functional: it complements all meiotic defects of *sme4Δ* and does not alter WT meiosis or sporulation. Thus, WT and *sme4Δ* strains carrying an ectopic copy of Sme4-GFP both produce 99% eight-spored asci, with 100% viable ascospores, like WT. Furthermore, the same pattern of Sme4-GFP localization is seen in both *sme4Δ* and WT backgrounds, implying that the fusion protein faithfully reports WT Sme4 localization. No GFP immunostaining is detectable in strains lacking the GFP fusion proteins, implying complete specificity for the tagged molecules. Unfortunately, all efforts to express the GFP-tagged versions of Podospora PaMe4 were unsuccessful.

Recombination Frequency Assays of Podospora. To associate the Δ*pame4::hygR* allele with chromosome 1 from the *T*-strain genetic background, we crossed a Δ*pame4::hygR* strain with the *PaMe4*$^+$ TS33 strain (Fig. S2). The TS33 strain is a haploid F1 offspring issued from a cross between *PaMe4*$^+$ *S* and *PaMe4*$^+$ *T* that harbors a chromosome 1 with *T* alleles for all of the 23 molecular markers tested (4). In the progeny of a Δ*pame4::hygR* strain crossed with the TS33 strain, we then selected a homokaryotic strain carrying both the *PaMe4* deleted allele and a chromosome 1 showing *T* alleles only (Δ*pame4::hygR* Chr1T) (Fig. S2). The same strategy was used to construct a strain harboring both the *PaMe4*

deleted allele and a chromosome 6 showing *T* alleles only (Δ*pame4::hygR* Chr6T), except that the Δ*pame4::hygR* strain was now crossed with the *PaMe4*$^{+}$ TS43 strain. Mycelia derived from ascospores collected from the crosses Δ*pame4::hygR* Chr1T X Δ*pame4::hygR* Chr1S and Δ*pame4::hygR* Chr6T X Δ*pame4::hygR* Chr6S were blended, and the resulting fragments were plated onto hygromycin-containing medium for regeneration. Among the regenerated mycelia, 62 were homokaryotic and therefore, formally haploid. PCR amplifications were performed according to the method used in ref. 4. Molecular makers were PCR-amplified with fluorescent primers (WellRED Oligos; Beckman Coulter) and analyzed using an automate sequencer (CEQ 8000; Beckman Coulter) according to the manufacturer's procedures.

SI Results

Phenotypes of *pame4* and *sme4* Null Alleles During the Vegetative Cycle. In both organisms, the null mutation is recessive in heterozygous crosses. Furthermore, full complementation was found when the Podospora *PaMe4* gene was introduced into the *pame4Δ* strain and when the Sordaria *SME4* gene was introduced in the *sme4Δ* strain. Moreover, although PaMe4 shows only 19% identity with the Sordaria Sme4 protein, the Sordaria WT *SME*4 gene restores an almost WT sporulation in the Podospora *pame4Δ* mutant (85% of four-spored asci in each perithecium), indicating corresponding functions. Correspondingly, the *PaMe4* gene restores sporulation in the Sordaria *sme4Δ* mutant.

Phylogenetic analyses reveal that the protein is well-conserved only among the Sordariales (e.g., Podospora, Sordaria, Neurospora, Chaetomium, Sporotrichum, and Thielavia species) (Fig. S1). Furthermore, the rather low percentage of identity found between Sordariale proteins (e.g., 19% between Sme4 and PaMe4 and 25% between *Neurospora crassa* NCU10217 and PaMe4) points to rapid evolution of the protein. NCU10217 and Sme4 exhibit 60% identity, reflecting the overall proximity between *S. macrospora* and *N. crassa* (5).

Deletion mutant phenotypes show that PaMe4 and Sme4 are not of central importance for the vegetative cycle; *pame4Δ* and *sme4Δ* mutants exhibit vegetative growth rates (measured by mycelial growth per 12 h) that are very similar to WT Podospora and Sordaria, respectively. However, *pame4Δ* mutants do show a shortened life span. In WT Podospora, senescence appears after 9.5 ± 1.74 cm growth in race tubes (expressed by an increase of the mycelial pigmentation and cellular death; reviewed in ref. 6); in *pame4Δ* mutant strains issued from the same cross, senescence appears earlier at 6.0 ± 2.58 cm. Neither Sordaria WT nor Sordaria *sme4Δ* shows senescence. In contrast, both deletion mutants exhibit major defects during sporulation. In Sordaria, only 1.5% eight-spored asci are seen in the mutant fruiting bodies compared with 99% eight-spored asci seen in WT. Similar reduction to ~1.2% of WT-like asci is observed in Podospora *pame4Δ* homozygous crosses (n = 100 and ~100 asci are in each fruiting body).

1. Marcou D (1979) Dominant enhancer effect of the meiotic *mei4* mutant on recombination frequencies restricted to linkage group VI in Podospora anserina. *Mol Gen Genet* 173:299–305.
2. Marcou D, Masson A, Simonet JM, Piquepaille G (1979) Evidence for non-random spatial distribution of meiotic exchanges in *Podospora anserina*: Comparison between linkage groups 1 and 6. *Mol Gen Genet* 176:67–79.
3. Simonet JM, Zickler D (1972) Mutations affecting meiosis in *Podospora anserina*. I. Cytological studies. *Chromosoma* 37:327–351.
4. Espagne E, et al. (2008) The genome sequence of the model ascomycete fungus *Podospora anserina*. *Genome Biol* 9:R77.
5. Nowrousian M, et al. (2010) De novo assembly of a 40 Mb eukaryotic genome from short sequence reads: *Sordaria macrospora*, a model organism for fungal morphogenesis. *PLoS Genet* 6:e1000891.
6. Jamet-Vierny C, Rossignol M, Haedens V, Silar P (1999) What triggers senescence in *Podospora anserina? Fungal Genet Biol* 27:26–35.

Fig. S1. Maximum likelihood phylogenetic tree of closely related *PaMe4/SME4* genes. Clear orthologs were found in the genomes of the following Sordariales: *Chaetomium globosum* (CHG09188.1), *Sporotrichum thermophile* (Spoth1_29412), *Thielavia terrestris* (Thite1_123493), *Neurospora crassa* (NCU10217), *N. discreta* (Neudi1_111487), and *N. tetrasperma* (Neute1_133090). Potential orthologs are present in fungi more distantly related, such as *Magnaporthe grisea* (MGG_12819), a Magnapothaceae, and hypocrealan fungi, including *Fusarium graminearum* (FG08441.1) and *Trichoderma reesei* (Tri_109189). The statistical support for actual orthology of PaMe4 with putative orthologs of the latter fungi is low; however, positions of the two *P. anserina* introns are conserved in the *F. graminearum* ortholog, arguing for common origin.

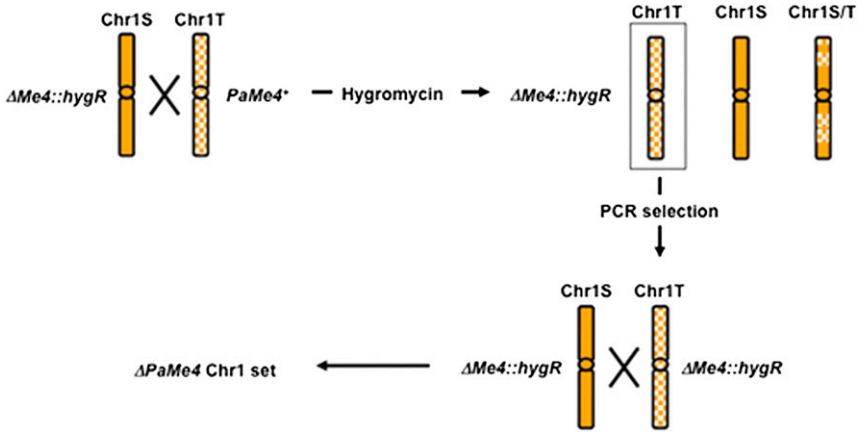

Fig. S2. Construction of the F1 populations used to assay recombination along Podospora chromosomes 1 and 6.

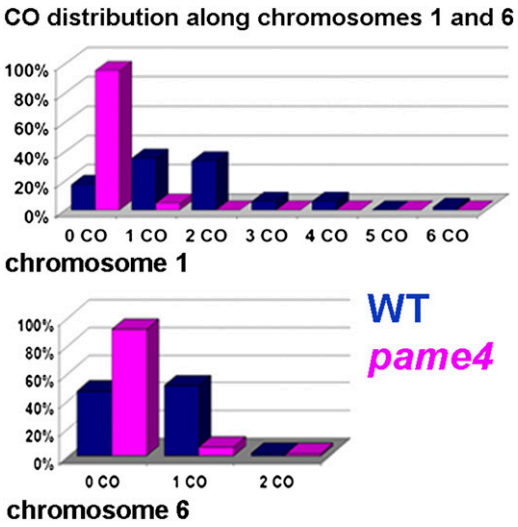

Fig. S3. Cross-over rates along chromosomes 1 and 6. Histograms (blue, WT; magenta, *pame4*) indicate the distribution of COs among the tested chromatids. The CO distribution along chromosomes is reported by the genotypes of haploid F1 progeny issued from a cross between polymorphic *PaMe4 S* and *PaMe4 T* strains (*Materials and Methods* and Fig. S2). Recombination was analyzed using 23 molecular markers scattered along chromosome 1 and 14 molecular markers scattered along chromosome 6. Along the long metacentric chromosome 1 (*Upper*), among 51 analyzed WT chromatids, 18 exhibited one CO, 17 exhibited two COs, 3 exhibited three COs, 3 exhibited four COs, 1 exhibited six COs, and 9 showed zero COs. In total, these 79 COs correspond to 1.5 COs per chromatid and thus, ~3 CO per meiosis along chromosome 1 (two chromatids). Along acrocentric chromosome 6, which is one-half the size of chromosome 1 (*Lower*), one-half of the 51 analyzed chromatids showed only one CO, one showed two COs, and 24 showed zero COs. In total, the 28 COs correspond to ~1.1 COs along this chromosome. In the absence of *PaMe4,* the number of COs is dramatically reduced (magenta histograms). Among 62 analyzed chromatids of chromosome 1, only three exhibited one CO, and zero presented multiple COs, which corresponds to ~0.1 COs per chromosome 1 and 0.006 CO/Mb. Similarly, among the 61 analyzed chromatids of chromosome 6, 56 showed zero COs, four exhibited one CO, and one showed two COs, which corresponds to ~0.2 COs per chromosome 6 and 0.0245 CO/Mb.

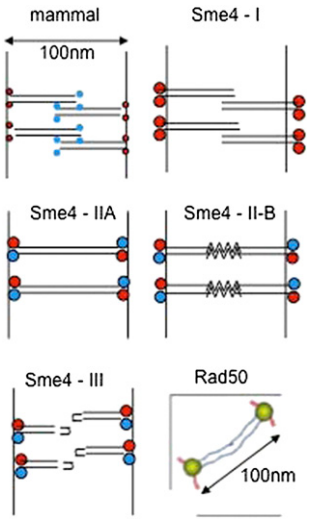

Fig. S4. Speculative models for Sme4 localization in the synaptonemal complex (SC) central region. (*Top Left*) In the mammal SC central region, synaptonemal complex protein 1 (SYCP1) transverse filament (TF) SYCP1 TF homodimers are attached by their C terminus (red circle) to the SC axial element, and they interact with their N terminus (blue circle) with the TF molecules attached to the homolog chromosome. (*Top Right*) Equivalent model (Sme4–I) for Sme4 location. (*Middle Left*) According to the large size of the Sme4 coiled-coil region (compared with Zip1 or SYCP1) (Table S1) and the fact that both N and C termini of Sme4 contain S/TPXX motifs, homodimers of Sme4 could span the 100-nm distance between the synapsed homologs. (*Middle Right*) Sme4 could also fold back on itself with the hinge domain extended in the central region. (*Bottom Left*) Sme4 homodimers might span one-half the distance with their central hinges linked by other SC central components homolog to those found in mammals central regions. (*Bottom Right*) This latter model is predicted by the behavior of Rad50, which links two sister DNAs at a distance of 100 nm (1).

1. Moreno-Herrero F, et al. (2005) Mesoscale conformational changes in the DNA-repair complex Rad50/Mre11/Nbs1 upon binding DNA. *Nature* 437:440–443.

Table S1. Comparison of Sme4 with the known SC TF proteins (1–9) and the SMC3 proteins of budding yeast and Sordaria

			Size (amino acids)							π					
	Organism	Width of the SC central space (nm)	Entire molecule	N end	C end	α-Helical domain	Coiled coil 1	Hinged	Coiled coil 2	N end	C end	Coiled coil	Entire molecule	S/TPXX repeat in C end	S/TPXX repeat in N end
Zip1	*S. cerevisiae*	115	875	184	126	565	143	76	346	4, 69	10, 09	6, 05	6, 4	3; 0 = 3	1; 0 = 1
Zyp1a	*Arabidopsis thaliana*	100–120	871	42	168	661	532	102	27	10, 17	9, 85	5, 2	5, 84	1; 3 = 4	0; 0 = 0
Zyp1b	*A. thaliana*	100–120	856	42	153	661	532	102	27	9, 99	9, 3	5, 39	5, 9	1; 2 = 3	0; 0 = 0
Zep1	*Orysa. sativa*	100–120	869	57	134	678	546	57	75	10, 12	9, 64	5, 22	5, 88	2; 0 = 2	0; 0 = 0
SYCP1	*Human*	100	976	123	199	674	578	34	62	5, 86	9, 73	5, 29	5, 78	0; 5 = 5	0; 0 = 0
Sycp1	*Rattus. novegicus*	100	946	58	148	700	605	44	51	4, 6	9, 85	5, 29	5, 56	1; 6 = 7	0; 0 = 0
Sycp1	*Mus. musculus*	100	993	105	185	674	578	34	62	5, 3	9, 78	5, 3	5, 69	1; 5 = 6	0; 0 = 0
SCP1	*Oryzias. latipes*	135	895	119	178	598	58	64	476	7, 7	10, 2	5, 24	6, 18	2; 5 = 7	2; 0 = 2
XP684182	*Danio. rerio*	135	1,000	112	188	700	53	61	586	9, 41	10, 13	5, 32	6, 54	3; 0 = 3	1; 6 =7
SYP-1	*C. elegans*	90–125	489	145	83	261	132	51	78	*	*	*	*		
C(3)G	*Drosophila*	109	744	156	93	395	395	0	0	9, 96	9, 73	4, 96	5, 92	0; 0 = 0	2; 1 = 3
Sme4	*S. macrospora*	100	1,643	514	409	720	214	125	381	9, 29	8, 79	5, 67	6, 63	2; 3 = 5	7; 4 = 11
Pame4	*P. anserina*	100	1,503	411	394	698	201	124	373	9, 65	9, 7	5, 18	6, 52	7; 6 = 13	9; 2 = 11
Ncme4	*N. crassa*	100	1,463	522	270	671	215	168	288	9	8, 9	5, 82	6, 9	2; 2 = 4	6; 2 = 8
SMC3	*S. cerevisiae*		1,230	176	187	867	316	203	440	7, 95	4, 96	5, 64	5, 63	0; 0 = 0	1; 0 = 1
SmSMC3	*S. macrospora*		1,199	176	187	836	328	156	352	8, 75	4, 75	6, 05	6, 04	1; 0 = 1	0; 0 = 0

*Probably not TF protein (4).

1. Dong HJ, Roeder GS (2000) Organization of the yeast Zip1 protein within the central region of the synaptonemal complex. *J Cell Biol* 148:417–426.
2. Higgins JD, Sanchez-Moran E, Armstrong SJ, Jones GH, Franklin FC (2005) The Arabidopsis synaptonemal complex protein ZYP1 is required for chromosome synapsis and normal fidelity of crossing over. *Genes Dev* 19:2488–2500.
3. de Boer E, Heyting C (2006) The diverse roles of transverse filaments of synaptonemal complexes in meiosis. *Chromosoma* 115:220–234.
4. Colaiácovo MP (2006) The many facets of SC function during *C. elegans* meiosis. *Chromosoma* 115:195–211.
5. Iwai T, et al. (2006) Structural components of the synaptonemal complex, SYCP1 and SYCP3, in the medaka fish *Oryzias latipes*. *Exp Cell Res* 312:2528–2537.
6. Jeffress JK, et al. (2007) The formation of the central element of the synaptonemal complex may occur by multiple mechanisms: The roles of the N- and C-terminal domains of the Drosophila C(3)G protein in mediating synapsis and recombination. *Genetics* 177:2445–2456.
7. Page SL, et al. (2008) Corona is required for higher-order assembly of transverse filaments into full-length synaptonemal complex in Drosophila oocytes. *PLoS Genet* 4:e1000194.
8. Bolcun-Filas E, et al. (2009) Mutation of the mouse Syce1 gene disrupts synapsis and suggests a link between synaptonemal complex structural components and DNA repair. *PLoS Genet* 5:e1000393.
9. Wang M, et al. (2010) The central element protein ZEP1 of the synaptonemal complex regulates the number of crossovers during meiosis in rice. *Plant Cell* 22:417–430.